Carbohydrate Polymers 155 (2017) 146–151

Contents lists available at ScienceDirect

Carbohydrate Polymers

journal homepage: www.elsevier.com/locate/carbpol

Silk fibroin organization induced by chitosan in layer-by-layer films: Application as a matrix in a biosensor

Jorge A.M. Delezuk[a,*], Adriana Pavinatto[a], Marli L. Moraes[b], Flávio M. Shimizu[a], Valquíria C. Rodrigues[a], Sérgio P. Campana-Filho[c], Sidney J.L. Ribeiro[d], Osvaldo N. Oliveira Jr.[a]

[a] São Carlos Institute of Physics, University of São Paulo (USP), CP 369, 13560-970, São Carlos, SP, Brazil
[b] Institute of Science and Technology at the Federal University of São Paulo (UNIFESP), 330 Talim Street, São José dos Campos, SP, Brazil
[c] São Carlos Institute of Chemistry, University of São Paulo (USP), CP 780, 135660-970, São Carlos, SP, Brazil
[d] Institute of Chemistry, São Paulo State University (UNESP), CP 355, 14801-970, Araraquara, SP, Brazil

ARTICLE INFO

Article history:
Received 2 June 2016
Received in revised form 16 August 2016
Accepted 17 August 2016
Available online 19 August 2016

Keywords:
Chitosan
Silk fibroin
Layer-by-layer
Biosensor

ABSTRACT

In this paper, we show that chitosan may induce conformation changes in silk fibroin (SF) in layer-by-layer (LbL) films, which were used as matrix for immobilization of the enzyme phytase to detect phytic acid. Three chitosan (CH) samples possessing distinct molecular weights were used to build CH/SF LbL films, and a larger change in conformation from random coils to β-sheets for SF was observed for high molecular weight chitosan (CHH). The CHH/SF LbL films deposited onto interdigitated gold electrodes were coated with a layer of phytase, with which phytic acid could be detected down to 10^{-9} M using impedance spectroscopy as the principle of detection and treating the data with a multidimensional projection technique. This high sensitivity may be ascribed to the suitability of the CHH/SF matrix, thus indicating that the molecular-level interactions between chitosan and SF may be exploited in other biosensors and biodevices.

1. Introduction

The immobilization of active biomolecules on solid surfaces is one of the most important challenges in the design and fabrication of biosensors, (Putzbach & Ronkainen, 2013) since a high performance in terms of sensitivity and selectivity depends on preserved bioactivity. In this context, the layer-by-layer (LbL) film-forming method has been proven excellent because it may lead to a suitable matrix as well as an active layer (Ariga, Hill, & Ji, 2007), mostly because entrained water in the film assists in keeping the native structure of the biomolecules (Siqueira, Caseli, Crespilho, Zucolotto, & Oliveira, 2010). The LbL film-forming method was originally conceived for the alternate deposition of oppositely charged polyelectrolytes (Decher & Schlenoff, 2002), but it has now been extended to a whole variety of other materials, and it may also be based on hydrophobic (Wong et al., 2012), hydrogen bonds (Kharlampieva, Kozlovskaya, & Sukhishvili, 2009) and covalent bonds (Fadeev & McCarthy, 2000). Many have been the materials used as matrix for immobilizing biomolecules in LbL films, but perhaps one could single out natural polymers and biomaterials (Li, Wang, & Sun, 2012), especially because they tend to be suitable scaffolds for the biomolecules. For instance, silk fibroin in β-sheet conformation has been used to enhance the analyte adsorption in biosensors produced with LbL films (Moraes, Lima, Silva, Cavicchioli, & Ribeiro, 2013).

Silk fibroin (SF), derived from *Bombyx mori* cocoons, is a widely used protein with remarkable mechanical properties (Bhardwaj & Kundu, 2011), in addition to being biocompatible (Rockwood et al., 2011). In contrast to other proteins, SF is characterized by Ala-Gly-X primary sequence, leading to regular conformations at its primary level (Altman et al., 2003). The repeating region for silk fibroin comprises various units, including highly repetitive GAGAGS hexamer and less repetitive GAGAGY (the less organized sequence) or/and AGVGYGAG motifs (Ha, Gracz, Tonelli, & Hudson, 2005). It may adopt different conformations, including random coils and β-sheets (Magoshi, Magoshi, & Nakamura, 1993). The latter (β-sheets) display improved properties in terms of degradation rate (Hu, Zhang, You, Wang, & Li, 2012), thermal stability (Moraes, Nogueira, Weska, & Beppu, 2010) and mechanical performance (Numata & Kaplan, 2010). SF has already been used in LbL films of different

* Corresponding author.
E-mail address: delezuk@gmail.com (J.A.M. Delezuk).

http://dx.doi.org/10.1016/j.carbpol.2016.08.060
0144-8617/

materials (Altman et al., 2003; Moraes et al., 2013; Shang, Zhu, & Fan, 2013), including with chitosan (Nogueira et al., 2010) which is a polycation in slightly acidic solutions, non-toxic, biocompatible and biodegradable. Chitosans have been exploited in biomedical and pharmaceutical applications as biomaterials as well as components of biodevices (Bégin & Van Calsteren, 1999; Kumar, 2000; Rinaudo, 2006). The solubility in water and biological activity of chitosans are governed by structural and physicochemical characteristics. Because the latter can be varied and tuned by changing molecular weight and average degree of acetylation, chitosans can actually be tailored for specific applications. In biosensors, for instance, chitosans have been shown excellent as matrices (Suginta, Khunkaewla, & Schulte, 2013). It is clear therefore that combining SF and chitosan in a matrix may result in improved performance in biosensing.

The main goal in this study is to verify whether synergy may be established with SF and chitosan of different molecular weights. The working hypothesis is that by using chitosan one may induce order in SF molecules, which would then be an optimized matrix for a biosensor. This was tested by fabricating multilayered SF/chitosan LbL films onto which a layer of the enzyme phytase was adsorbed to detect phytic acid using impedance spectroscopy as the principle of detection. The most common procedures to determine phytic acid concentration are precipitation with iron (III) followed by titration analysis (Wu, Tian, Walker, & Wang, 2009), nuclear magnetic resonance spectroscopy (O'Neill, Sargent, & Trimble, 1980) and high-performance liquid chromatography (Lehrfeld, 1994). Phytic acid has also been detected with biosensors containing immobilized phytase in layer-by-layer (LbL) films (Moraes, Oliveira, Filho, & Ferreira, 2008). Amperometric biosensors have reached a detection limit of 2.0×10^{-3} mmol L^{-1} (Mak, Ng, Chan, Kwong, & Renneberg, 2004), while a biosensor based on impedance spectroscopy has allowed a detection limit for phytic acid of 10^{-6} mol L^{-1} (Moraes, Maki et al., 2010). Our sensing data were obtained with a selected film architecture, which was determined in a systematic characterization of SF/chitosan films using UV–vis spectroscopy, fluorescence spectroscopy, circular dichroism, contact angle measurements and polarization-modulated infrared reflection absorption spectroscopy (PM-IRRAS).

2. Experimental

2.1. Silk fibroin

Silk fibroin (SF) was extracted from the cocoons of *Bombyx mori* silkworm supplied by Bratac SA, Brazil. 10 g of cocoons were boiled during 30 min in 2 L of 0.02 M Na_2CO_3 solution to remove sericin. For each 10 g of the silk yarn, 100 mL of $CaCl_2/CH_3CH_2OH/H_2O$ (1:2:8) solution were added and heated to 60 °C for dissolution. This solution was then dialyzed against deionized water using a cellulose acetate membrane at room temperature for 48 h. SF was then centrifuged three times at 20,000 rpm for 30 min at 5 °C to remove impurities and aggregates (Rockwood et al., 2011). The final concentration of SF in solution was 3.5% in weight.

2.2. Chitosans

Three chitosans with distinct weight average molecular weights were used to build up chitosan/silk fibroin films: (i) high-molecular weight (CHH) obtained by deacetylation of β-chitin by using ultrasound irradiation (Delezuk, Cardoso, Domard, & Campana-Filho, 2011), (ii) medium-molecular weight (CHM) purchased from Polymar-Brazil and iii) chitosan oligosaccharide (CHL) from Kitto Life-South Korea. The average degree of acetylation (DA) of the chitosans was determined using ^{1}H NMR spectroscopy while the weight average (Mw) was determined by size exclusion chromatography (SEC) in a Shimadzu (CTO-10A), RID – 6A equipment, using Shodex Ohpak SB-G (50 mm × 6 mm – pre column) + Shodex Ohpak SB-803-HQ (8 mm DI × 300 mm) + Shodex Ohpak SB-805-HQ (8 mm DI × 300 mm) columns, refractive index detector, flow rate 0.6 mL min-^{1} and sample concentration of 4 mg mL^{-1} in acetic acid buffer as solvent at 35 °C (Pavinatto et al., 2013). The results of DA and Mw chitosans are given in Table 1.

Table 1
Weight average molecular weight (Mw) and average degree of acetylation (DA) of chitosan samples used to build LbL films.

Chitosan	Mw (g mol^{-1})	DA (%)
CHH	470,900 ± 2000	13.6 ± 0.3
CHM	136,000 ± 1200	14.0 ± 0.5
CHL	2561 ± 110	11.0 ± 0.6

2.3. Layer-by-layer films

SF was found to adopt β-sheet structures in chitosan/SF films (Chen, Li, & Yu, 1997) for a 1:9 SF:chitosan ratio, which was also used here with an aqueous SF solution (pH 5.6) at a concentration of 0.025% (w/v) and chitosan solution in 0.3 M acetic acid/0.2 M sodium acetate buffer (pH 4.5) at 0.225% (w/v). The choice of a 1:9 SF:chitosan ratio does not mean that this is the final composition in the LbL films, since adsorption governed by electrostatic interactions ceases when there is charge compensation. Chitosan/SF films were deposited onto quartz substrates previously treated with 1:1:5 solution of NH_4OH:H_2O_2:H_2O for 10 min at 70 °C, and then with a 1:1:6 solution of HCl: H_2O_2:H_2O for 10 min at 70 °C. The deposition process was carried out by immersing the substrate in chitosan solution for 10 min and in SF solution for 10 min. After each step of deposition, the film was washed with deonized water (twice) to remove poorly adsorbed molecules and dried gently with constant flowing nitrogen. The multilayer deposition was monitored by UV–vis and fluorescence spectroscopy, performed with a U-2900 UV–vis spectrophotometer from Hitachi and RF-5301PC spectrofluorimeter from Shimadzu, respectively. The film thickness was measured using Veeco Dektak 150 Surface Profilometer, and the values reported are taken as the average from four measurements.

Contact angle measurements were carried out in a KSV system (KSV, Finland). A drop of water (10 μL) was deposited on the film surface and the drop shape was recorded by a digital CCD camera (LG). The acquired image was analyzed using KSV software, from which the evolution of the contact angle as a function of time was determined. The value of the contact angle was taken as the average from at least three measurements, after 15 s of the water being dripped to reach equilibrium, made on different areas of the film surface. The PM-IRRAS analysis was carried out using a KSV PMI550 instrument (KSV, Finland), with spectral resolution of 8 cm^{-1}. The light beam reached the film at 81°, being continuously modulated between *s*- and *p*-polarizations at a high frequency. This allows for the simultaneous measurement of the spectra for the two polarizations. The difference spectrum provides surface-specific information on oriented moieties, while the sum gives the reference spectrum. In addition, with the simultaneous measurements, the effect of water vapor is reduced. Circular dichroism (CD) spectra of SF aqueous solutions were collected with a quartz cell of 1 mm optical path length. The CD spectra of chitosan/SF films were measured directly over the films deposited on quartz substrates, with the optical path being given by the film thickness. Measurements were performed on a J-815 Circular Dichroism Spectrometer (Jasco Inc., Tokyo, Japan), with the bandwidth of 1 nm, a response

Table 2
Thickness of LbL films made with 5, 7 and 9 bilayers of SF and chitosans of different molecular weights (CHL, CHM and CHH).

Number of Bilayers	Thickness (nm)		
	CHL/SF	CHM/SF	CHH/SF
5	31.61 ± 1.47	38.15 ± 1.98	48.00 ± 4.00
7	39.50 ± 2.00	56.28 ± 2.96	73.57 ± 5.47
9	66.56 ± 3.70	88.74 ± 4.43	102.7 ± 8.75

time of 0.5 s, and scanning speed of 100 nm/min. CD spectra were obtained by averaging six scans.

2.4. Biosensor

Impedance spectroscopy measurements were performed using interdigitated electrodes with gold tracks, with 10 μm spacing between tracks, covered with an LbL film containing five bilayers of CHH/SF and a top layer of phytase. Phytic acid in different concentrations (0, 10^{-2}, 10^{-3}, 10^{-4}, 10^{-5}, 10^{-6}, 10^{-7}, 10^{-8} and 10^{-9} M) dissolved in sodium acetate buffer 100 mM (pH 5.5) was used as analyte. The sensor data were treated with multidimensional projection techniques implemented in the PEx-Sensors software (Aoki et al., 2014).

3. Results and discussion

3.1. Effect of chitosan molecular weight on chitosan/SF LbL films

The effects of using the three distinct chitosan samples on LbL film growth and film properties were tested. Fig. 1 shows UV–vis absorption and fluorescence spectra used to monitor film growth. The absorption spectra exhibited a band at 280 nm, which is assigned to tyrosine (Tyr) residues from SF since chitosan does not absorb at this wavelength (see Fig. S1). The intensity of the 280 nm band increased monotonically with the number of bilayers for the CHL/SF and CHM/SF films, while a dip on the dependence with the number of bilayers occurred in CHH/SF films (Fig. 1a). This latter peculiar behavior was proven to be reproducible in various control experiments, and it is apparently related to molecular reorganization rather than desorption of material, since such a dip was not observed in the fluorescence data (Fig. 1b). In fact, taken together the results from Fig. 1a and b indicate that adsorption of CHH/SF was more efficient as compared to CHM/SF and CHL/SF. In particular, the fluorescence at 348 nm assigned to tryptophan (Try) residues from SF was considerably higher for CHH/SF, probably due to a larger percentage of Try groups being exposed in comparison to the LbL films with the other chitosans. Also worth noticing is the almost thickness-independent value of fluorescence emission for CHM/SF and CHL/SF films. Table 2 shows that the LbL films made with SF have increased thickness with increasing number of bilayers, as one should expect, while film thickness also increased with the chitosan molecular weight. Therefore, the organization of SF molecules seemed to vary with the molecular weight of the chitosan.

The effect of chitosan on molecular organization of SF was confirmed by circular dichroism (CD) measurements in Fig. 2. The CD spectrum of SF aqueous solution (0.025% (w/v)) displays a minimum at ca. 197 nm, which is characteristic of random coils. For SF adsorbed onto a solid substrate or in chitosans thin films, the β-sheet conformation was clearly formed with a minimum at about 217 nm. The conformational change can be attributed to molecular rearrangement due to immobilization in the films, particularly for the chitosan/SF film due to hydrogen bonding between protein (SF) and chitosan, in comparison with films formed only by SF. Furthermore, such behavior is more pronounced for CHH in the LbL films. Chitosan behaves as a semi-rigid rod and worm-like chain in

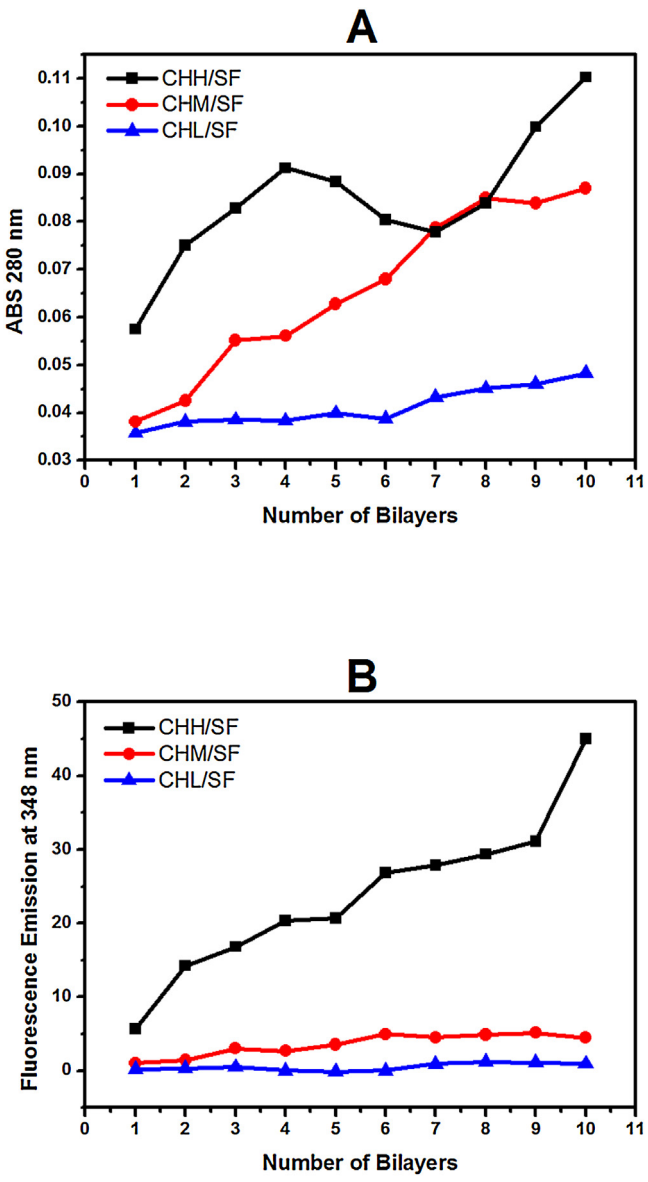

Fig. 1. (a) UV–vis absorption at 280 nm and (b) fluorescence emission at 348 nm, for CHH (■), CHM (●) and CHL (▲)/SF film as a function of deposited bilayers.

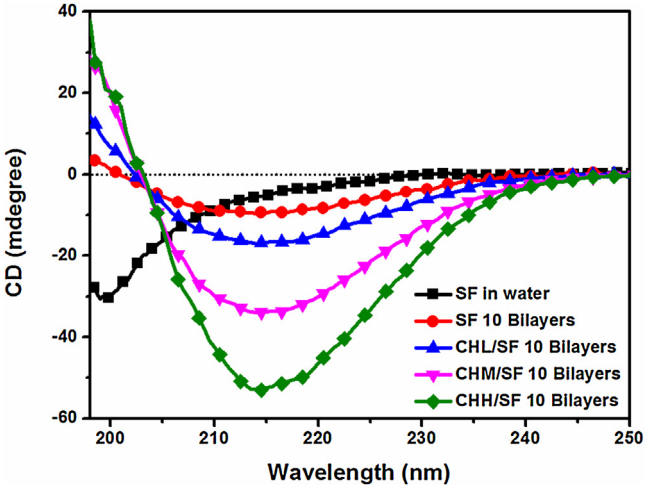

Fig. 2. Circular dichroism (CD) spectra for SF aqueous solution (■) and ten bilayers of SF (●), CHL/SF (▲), CHM/SF(▼) and CHH/SF (♦) in LbL films.

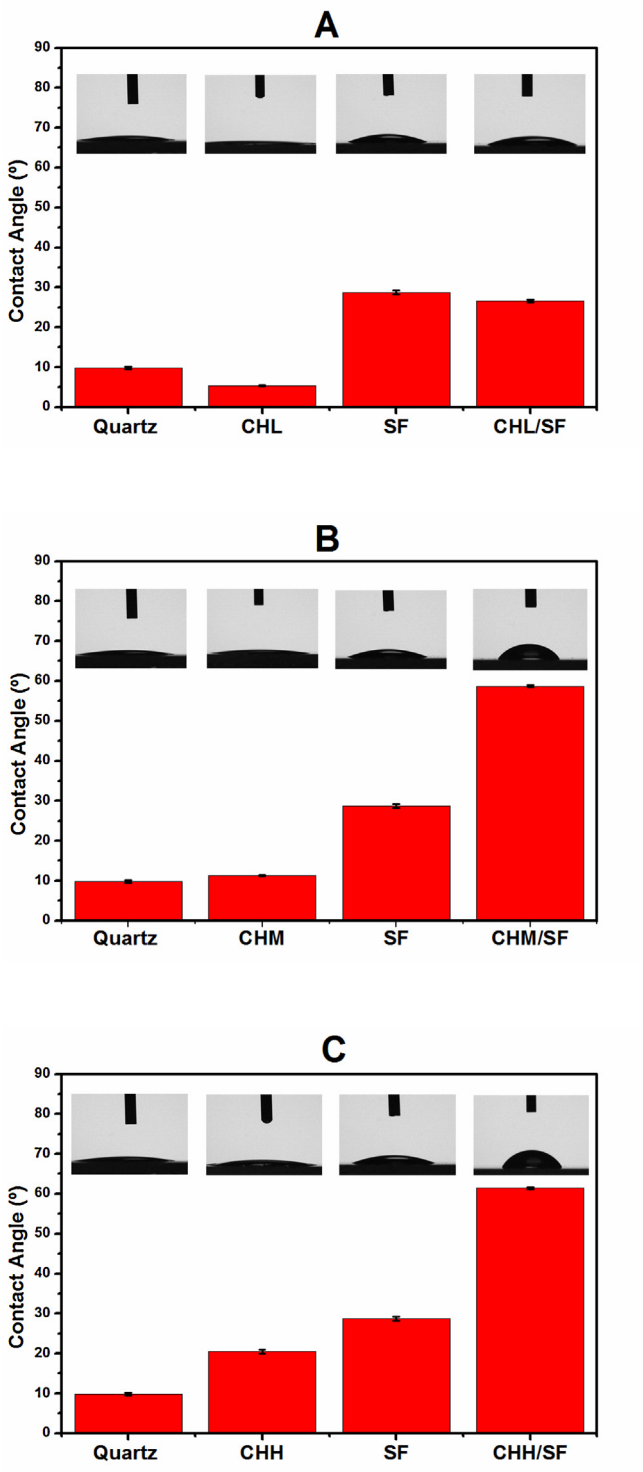

Fig. 3. Contact angle values and errors bars for various surfaces: quartz substrate, one-layer film of CHL (a), CHM (b) and CHH (c), one-layer film of SF and bilayers of CHL/SF, CHM/SF and CHH/SF. Inset: water drop images for each surface (on top).

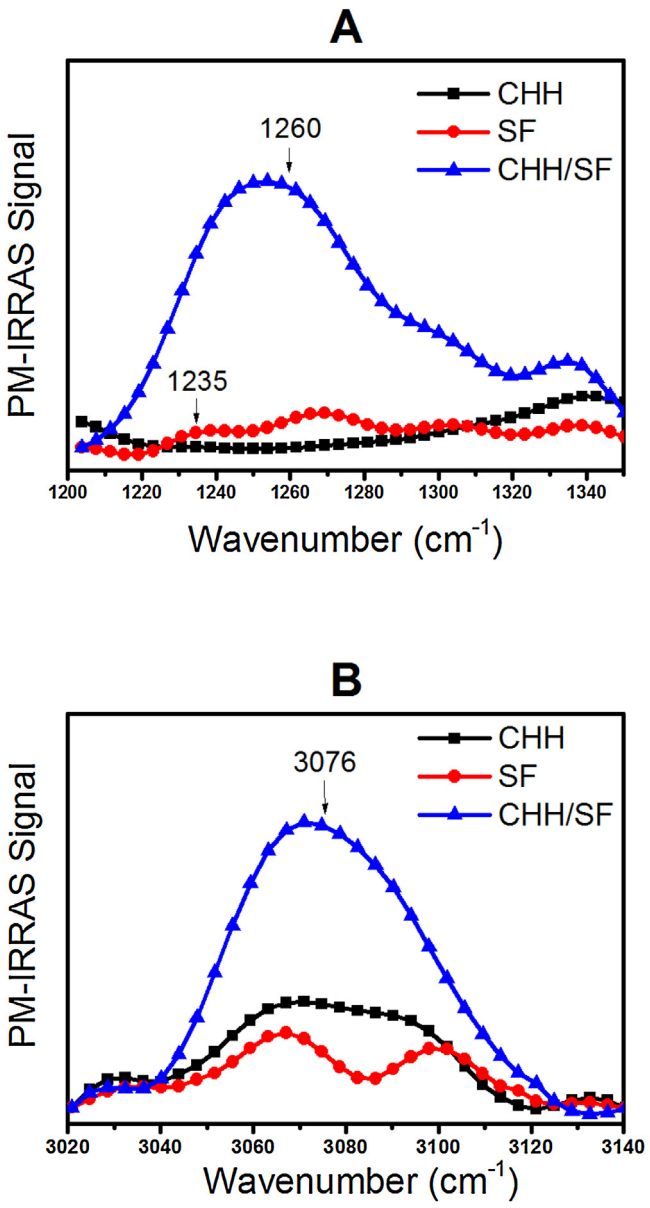

Fig. 4. PM-IRRAS spectra for CHH (■) and SF (●) one-layer films, and CHH/SF(▲) bilayer: (a) from 1200 cm^{-1} to 1350 cm^{-1} and (b) from 3020 cm^{-1} to 3140 cm^{-1}.

acetic acid/sodium acetate buffer (Morris, Castile, Smith, Adams, & Harding, 2009); when immobilized on a quartz substrate the chains remain extended, thus favoring β-sheet SF formation that increases with increasing molecular weight of chitosan.

The wettability of the LbL films was also affected by the type of chitosan used, as indicated in the changes in shape of the water drop during contact angle measurements for the various film surfaces in Fig. 3. The most hydrophilic surface was made with a layer of CHL, even more hydrophilic than quartz. This high affinity for water is manifested in the CHL/SF bilayer film, in this case with an intermediate hydrophilicity between CHL and SF films. Medium (CHM) and high (CHH) molecular weight chitosans promote increased hydrophobicity in the CH/SF films. The contact angle increased for CHM/SF (Fig. 3b) and CHH/SF (Fig. 3c) LbL films, suggesting that SF nonpolar residues (Try and Tyr) are probably oriented in the opposite direction to the chitosan substrate, thereby generating more hydrophobic and organized surfaces of SF. In subsidiary experiments we measured the contact angle of CH/SF films with larger numbers of bilayers (up to 10) and the overall behavior remained the same as for the bilayer films shown in Fig. 3.

The results presented so far indicate that CHH promotes orientation of SF in LbL films, with the non-polar Tyr and Try residues exposed on the film surface. This hypothesis was confirmed by taking the PM-IRRAS spectra of SF and CHH one-layer films and CHH/SF bilayer films deposited onto gold-coated glass slides. Indeed, Fig. 4 shows much more intense bands for the CHH/SF film, consistent with more organized SF molecules. In particular, a shift in amide III

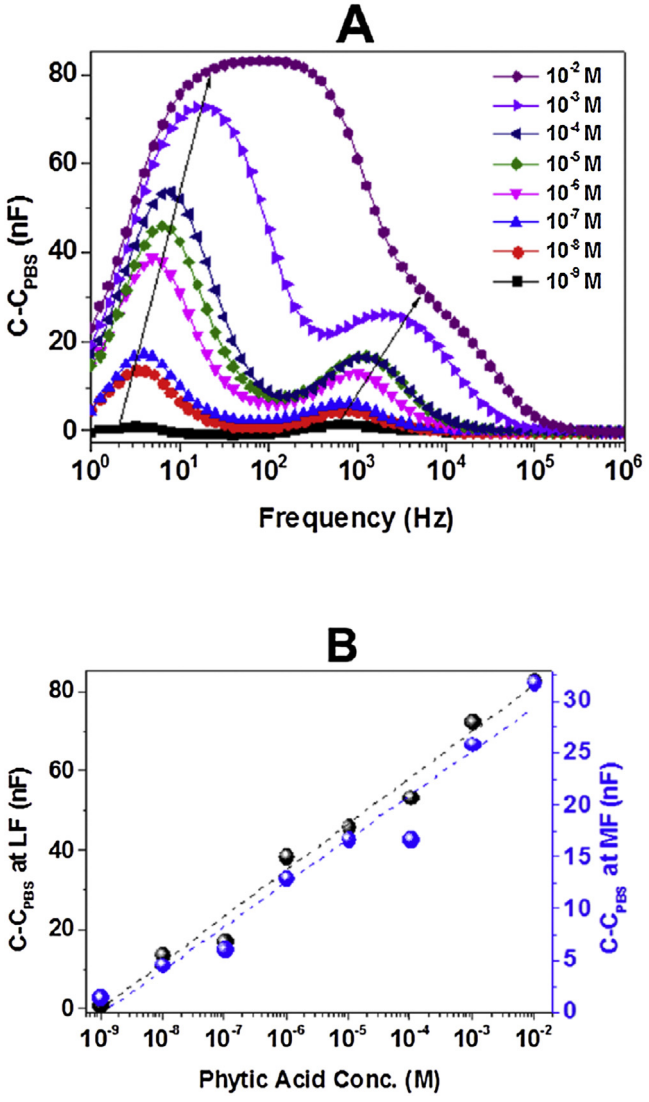

Fig. 5. (a) Difference in capacitance *versus* frequency of the coated electrode $(CHH/SF)_5$/Phytase at different concentrations of phytic acid (0, 10^{-2}, 10^{-3}, 10^{-4}, 10^{-5}, 10^{-6}, 10^{-7}, 10^{-8} and 10^{-9} M) and (b) maximum peak value vs. solution concentration at low frequencies (LF) and at intermediate frequencies (MF).

band in Fig. 4a was observed, from random coils at 1235 cm^{-1} for the SF film to β-sheets at 1265 cm^{-1} for the CHH/SF film. Moreover, the band at 3076 cm^{-1} assigned to tryptophan (Try) is much more intense in CHH/SF (Fig. 4b), suggesting that this residue is more exposed when chitosan is used as substrate for SF, as inferred from the contact angle results.

3.2. Application of CHH/SF film in a biosensor

Having found that CHH induces organization of SF in LbL films, we hypothesized that CHH/SF LbL films could be suitable matrices for immobilization of biomolecules in biosensors. In order to prove that, the enzyme phytase was adsorbed on a 5-bilayer CHH/SF LbL film to detect phytic acid. It should be mentioned that we did not perform a systematic search for the ideal chitosan/SF film architecture, but just assumed that CHH/SF would be adequate owing to the organization induced on SF. As for the number of bilayers, we chose a 5-bilayer film as the matrix because there is evidence in the literature that 3–5 bilayers is the ideal thickness for biosensing. The high sensitivity to be reported does prove that the architecture was adequate. Fig. 5a shows the difference in capacitance, i.e. the values measured with and without phytic acid in solution, vs frequency from 1 to 1 MHz. Two relaxation processes occur at low and intermediate frequencies. The low frequency process is assigned to an ionic relaxation resulting from accumulation of ions at the surface electrode (Maxwell–Wagner–Sillars polarization effect), forming the electrical double layer whose capacitance increases with the analyte concentration. The second process is attributed to a dipolar relaxation (Kremer & Schönhals, 2002) of permanent dipoles, and the peak increases with increasing analyte concentration due to the loss of dipole orientation because of further adsorption of the analyte onto the film. Fig. 5b shows that for both peaks the capacitance difference increases linearly with phytic acid concentration.

The whole spectra of normalized capacitance data for all the samples were analyzed using the multidimensional projection technique referred to as Interactive Document Map (IDMAP), implemented in the PEx-Sensors software, which has been successful in analyzing biosensing data (Soares, Shimizu et al., 2015; Soares, Soares et al., 2015; Soares et al., 2016). Dissimilarity was defined in terms of Euclidian distances between the signals. Fig. 6 shows the IDMAP plot, with clear discrimination of phytic acid solution at concentrations of 10^{-9} to 10^{-2} M and from PBS solution. This low detection limit of 10^{-9} mol L^{-1} indicates that the biosen-

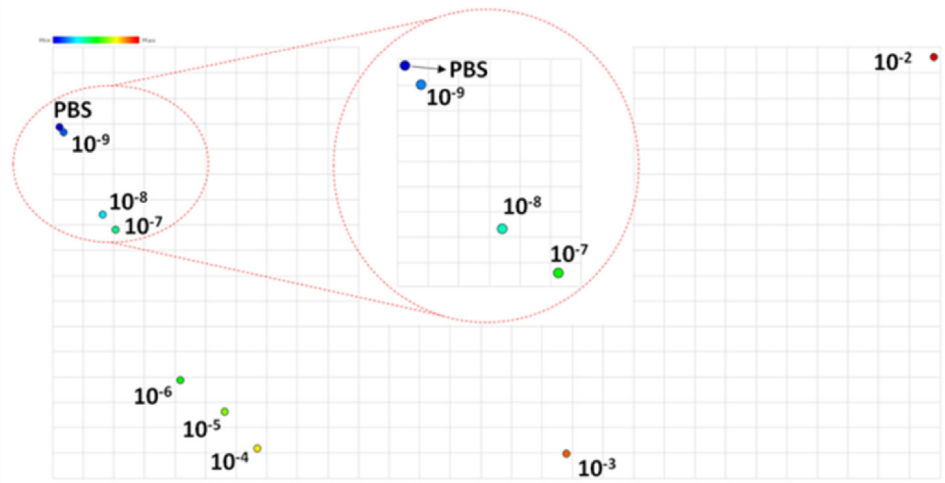

Fig. 6. IDMAP plot for the normalized capacitance vs. frequency curves for different concentrations of phytic acid. The zoomed image on the red-dashed circle shows discrimination of PBS solution from 10^{-2} to nM concentration of phytic acid. (For interpretation of the references to colour in this figure legend, the reader is referred to the web version of this article.)

sor made with CHH/SF LbL film is more sensitive than others found in the literature, e.g. 10^{-6} mol L^{-1} in (Moraes, Maki et al., 2010).

4. Conclusions

The molecular-level interactions, probably H-bonding, between chitosans and SF made it possible to build LbL films where the degree of SF organization could be varied. Particularly for the higher molecular weight chitosan (CHH), SF adopted a β-sheet conformation, as indicated by circular dichroism and large fluorescence emission of CHH/SF LbL films. Owing to this enhanced organization for SF, the CHH/SF LbL films were selected as matrix for immobilization of phytase, then used to detect phytic acid. Clear demonstration of a high sensitivity to phytic acid, down to nM level, was presented from the analysis of impedance spectroscopy data using the IDMAP projection technique. Furthermore, this sensitivity can in principle be improved if a full-fledged optimization procedure is performed with distinct architectures and number of bilayers. One may therefore conclude that the control of properties provided by the combination of chitosans and SF is promising for developing novel biosensors and biodevices requiring a suitable matrix.

Acknowledgments

The authors thank the Brazilian agencies FAPESP (2013/14262-7), CNPq, CAPES (Nanobiotec - 04/CII Program, 2008) for the financial support.

Appendix A. Supplementary data

Supplementary data associated with this article can be found, in the online version, at http://dx.doi.org/10.1016/j.carbpol.2016.08.060.

References

Altman, G. H., Diaz, F., Jakuba, C., Calabro, T., Horan, R. L., Chen, J., et al. (2003). Silk-based biomaterials. *Biomaterials*, *24*(3), 401–416.
Aoki, P. H. B., Alessio, P., Volpati, D., Paulovich, F. V., Riul, A., Jr., Oliveira, O. N., Jr., et al. (2014). On the distinct molecular architectures of dipping- and spray-LbL films containing lipid vesicles. *Materials Science and Engineering: C*, *41*, 363–371.
Ariga, K., Hill, J. P., & Ji, Q. (2007). Layer-by-layer assembly as a versatile bottom-up nanofabrication technique for exploratory research and realistic application. *Physical Chemistry Chemical Physics*, *9*(19), 2319–2340.
Bégin, A., & Van Calsteren, M.-R. (1999). Antimicrobial films produced from chitosan. *International Journal of Biological Macromolecules*, *26*(1), 63–67.
Bhardwaj, N., & Kundu, S. C. (2011). Silk fibroin protein and chitosan polyelectrolyte complex porous scaffolds for tissue engineering applications. *Carbohydrate Polymers*, *85*(2), 325–333.
Chen, X., Li, W., & Yu, T. (1997). Conformation transition of silk fibroin induced by blending chitosan. *Journal of Polymer Science: Part B: Polymer Physics*, *35*(14), 2293–2296.
Decher, G., & Schlenoff, J. B. (2002). *Multilayer thin films: sequential assembly of nanocomposite materials*. Weinheim, Germany: Wiley-VCH.
Delezuk, J. A. D. M., Cardoso, M. B., Domard, A., & Campana-Filho, S. P. (2011). Ultrasound-assisted deacetylation of beta-chitin: Influence of processing parameters. *Polymer International*, *60*(6), 903–909.
Fadeev, A. Y., & McCarthy, T. J. (2000). Self-assembly is not the only reaction possible between alkyltrichlorosilanes and surfaces: Monomolecular and oligomeric covalently attached layers of dichloro- and trichloroalkylsilanes on silicon. *Langmuir*, *16*(18), 7268–7274.
Ha, S. W., Gracz, H. S., Tonelli, A. E., & Hudson, S. M. (2005). Structural study of irregular amino acid sequences in the heavy chain of Bombyx mori silk fibroin. *Biomacromolecules*, *6*(5), 2563–2569.
Hu, Y., Zhang, Q., You, R., Wang, L., & Li, M. (2012). The relationship between secondary structure and biodegradation behavior of silk fibroin scaffolds. *Advances in Materials Science and Engineering*, *2012*, 1–5.
Kharlampieva, E., Kozlovskaya, V., & Sukhishvili, S. A. (2009). Layer-by-layer hydrogen-bonded polymer films: From fundamentals to applications. *Advanced Materials*, *21*(30), 3053–3065.
Kremer, F., & Schönhals, A. (2002). *Broadband dielectric spectroscopy*. Berlin: Springer.
Kumar, M. N. V. R. (2000). A review of chitin and chitosan applications. *Reactive and Functional Polymers*, *46*(1), 1–27.
Lehrfeld, J. (1994). HPLC separation and quantitation of phytic acid and some inositol phosphates in foods: Problems and solutions. *Journal of Agricultural and Food Chemistry*, *42*, 2726–2731.
Li, Y., Wang, X., & Sun, J. (2012). Layer-by-layer assembly for rapid fabrication of thick polymeric films. *Chemical Society Reviews*, *41*(18), 5998–6009.
Magoshi, J., Magosh, Y., & Nakamura, S. (1993). Mechanism of fiber formation of silkworm. *Silk Polymers*, *544*, 292–310. American Chemical Society
Mak, W. C., Ng, Y. M., Chan, C., Kwong, W. K., & Renneberg, R. (2004). Novel biosensors for quantitative phytic acid and phytase measurement. *Biosensors & Bioelectronics*, *19*(9), 1029–1035.
Moraes, M. L., Oliveira, O. N., Jr., Filho, U. P. R., & Ferreira, M. (2008). Phytase immobilization on modified electrodes for amperometric biosensing. *Sensors and Actuators B: Chemical*, *131*(1), 210–215.
Moraes, M. L., Lima, L. R., Silva, R. R., Cavicchioli, M., & Ribeiro, S. J. (2013). Immunosensor based on immobilization of antigenic peptide NS5A-1 from HCV and silk fibroin in nanostructured films. *Langmuir*, *29*(11), 3829–3834.
Moraes, M. L., Maki, R. M., Paulovich, F. V., Rodrigues Filho, U. P., de Oliveira, M. C. F., Riul, A., et al. (2010). Strategies to optimize biosensors based on impedance spectroscopy to detect phytic acid using layer-by-layer films. *Analytical Chemistry*, *82*(8), 3239–3246.
Moraes, M. A. D., Nogueira, G. M., Weska, R. F., & Beppu, M. M. (2010). Preparation and characterization of insoluble silk fibroin/chitosan blend films. *Polymers*, *2*(4), 719–727.
Morris, G. A., Castile, J., Smith, A., Adams, G. G., & Harding, S. E. (2009). Macromolecular conformation of chitosan in dilute solution: A new global hydrodynamic approach. *Carbohydrate Polymers*, *76*(4), 616–621.
Nogueira, G. M., Swiston, A. J., Beppu, M. M., & Rubner, M. F. (2010). Layer-by-layer deposited chitosan/silk fibroin thin films with anisotropic nanofiber alignment. *Langmuir*, *26*(11), 8953–8958.
Numata, K., & Kaplan, D. L. (2010). Silk-based delivery systems of bioactive molecules. *Advanced Drug Delivery Reviews*, *62*(15), 1497–1508.
O'Neill, I. K., Sargent, M., & Trimble, M. L. (1980). Determination of phytate in foods by phosphorus-31 Fourier transform nuclear magnetic resonance spectrometry. *Analytical Chemistry*, *52*(8), 1288–1291.
Pavinatto, A., Pavinatto, F. J., Delezuk, J. A. D. M., Nobre, T. M., Souza, A. L., Campana-Filho, S. P., et al. (2013). Low molecular-weight chitosans are stronger biomembrane model perturbants. *Colloids and Surfaces B: Biointerfaces*, *104*, 48–53.
Putzbach, W., & Ronkainen, N. J. (2013). Immobilization techniques in the fabrication of nanomaterial-based electrochemical biosensors: A review. *Sensors (Basel)*, *13*(4), 4811–4840.
Rinaudo, M. (2006). Chitin and chitosan: Properties and applications. *Progress in Polymer Science*, *31*(7), 603–632.
Rockwood, D. N., Preda, R. C., Yucel, T., Wang, X., Lovett, M. L., & Kaplan, D. L. (2011). Materials fabrication from Bombyx mori silk fibroin. *Nature Protocols*, *6*(10), 1612–1631.
Shang, S., Zhu, L., & Fan, J. (2013). Intermolecular interactions between natural polysaccharides and silk fibroin protein. *Carbohydrate Polymers*, *93*(2), 561–573.
Siqueira, J. R., Jr., Caseli, L., Crespilho, F. N., Zucolotto, V., & Oliveira, O. N., Jr. (2010). Immobilization of biomolecules on nanostructured films for biosensing. *Biosensors and Bioelectronics*, *25*(6), 1254–1263.
Soares, J. C., Soares, A. C., Pereira, P. A. R., Rodrigues, V. C., Shimizu, F. M., Melendez, M. E., et al. (2016). Adsorption according to the Langmuir–Freundlich model is the detection mechanism of the antigen p53 for early diagnosis of cancer. *Physical Chemistry Chemical Physics*, *18*, 8412–8418.
Soares, J. C., Shimizu, F. M., Soares, A. C., Caseli, L., Ferreira, J., & Oliveira, O. N., Jr. (2015). Supramolecular control in nanostructured film architectures for detecting Breast cancer. *ACS Applied Materials & Interfaces*, *7*(22), 11833–11841.
Soares, A. C., Soares, J. C., Shimizu, F. M., Melendez, M. E., Carvalho, A. L., & Oliveira, O. N., Jr. (2015). Controlled film architectures to detect a biomarker for pancreatic cancer using impedance spectroscopy. *ACS Applied Materials & Interfaces*, *7*(46), 25930–25937.
Suginta, W., Khunkaewla, P., & Schulte, A. (2013). Electrochemical biosensor applications of polysaccharides chitin and chitosan. *Chemical Reviews*, *113*(7), 5458–5479.
Wong, S. Y., Han, L., Timachova, K., Veselinovic, J., Hyder, M. N., Ortiz, C., et al. (2012). Drastically lowered protein adsorption on microbicidal hydrophobic/hydrophilic polyelectrolyte multilayers. *Biomacromolecules*, *13*(3), 719–726.
Wu, P., Tian, J.-C., Walker, C. E., & Wang, F.-C. (2009). Determination of phytic acid in cereals—a brief review. *International Journal of Food Science & Technology*, *44*(9), 1671–1676.